Vol. 1, No. 1 January 1991

GSA TODAY

A Publication of the Geological Society of America

INSIDE

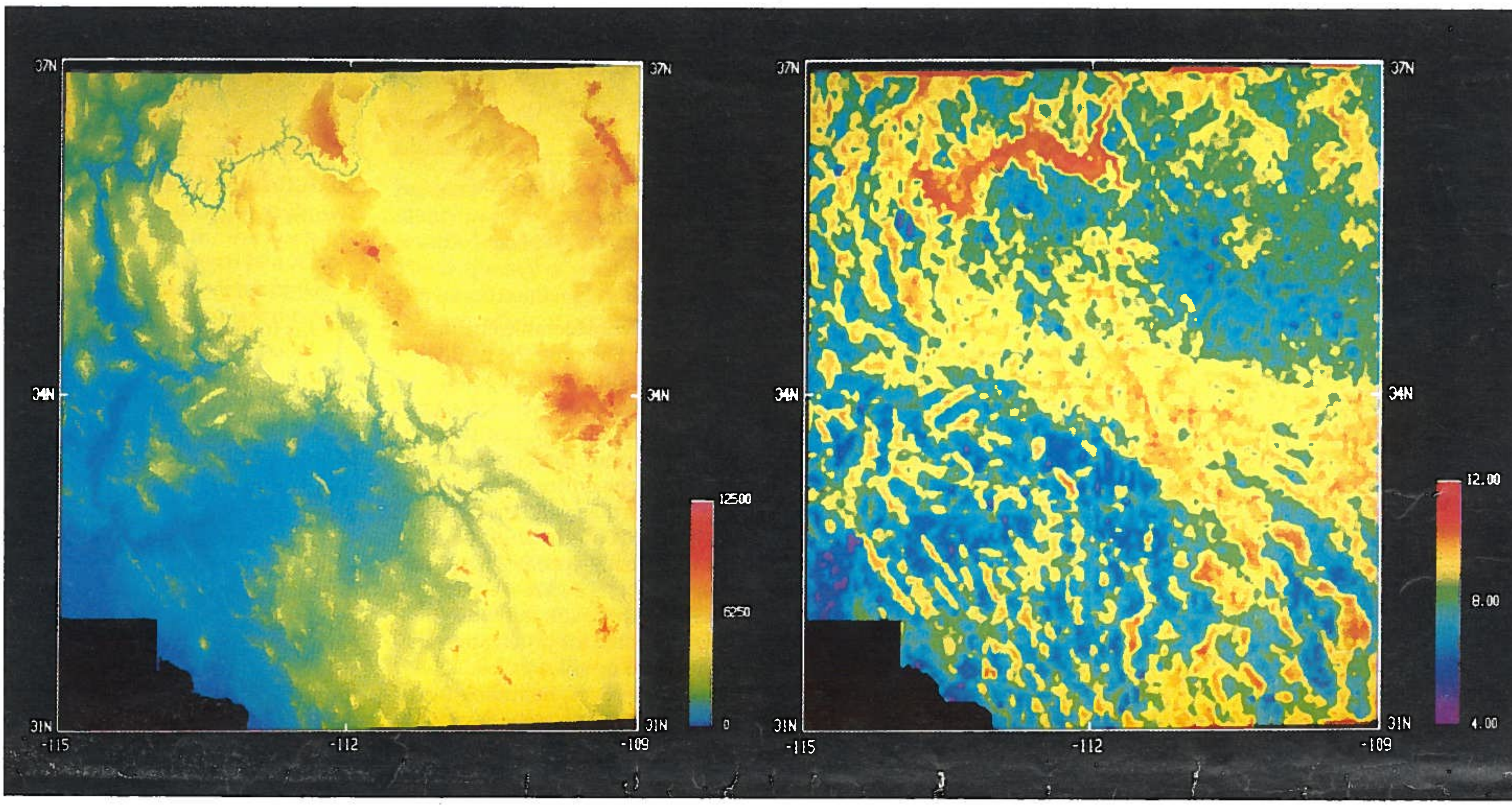

The photograph on the left is the color-coded elevation (in feet) of the state of Arizona. The photograph on the right is the color-coded roughness amplitudes (arbitrary units) of the state of Arizona.

Fractals in geology: What are they and what are they good for?

Donald L. Turcotte
Department of Geological Sciences
Cornell University, Ithaca, NY 14853

ABSTRACT
Objects that are scale invariant are fractals. Many geologic phenomena and processes are scale invariant and are therefore fractals. Rocky coastlines and river networks are examples. Statistical frequency-size distributions of economic ore deposits, earthquakes, and volcanoes are fractals. Fractals can be used in empirical correlations, but they are also associated with chaotic processes. There is considerable evidence that tectonics and erosion are examples of chaotic processes.

What is a Fractal?

I am sure that you have heard of fractals; you may have seen fractally generated computer graphics and synthetic landscapes or may be aware that a rocky coastline is a fractal. But are fractals more than a scientific curiosity? I would like to convince you that at the very least, fractals help us to bridge the gap between geostatistics and physical and chemical modeling of geologic processes.

I am often asked the question, "What is a fractal?" A definition that is generally applicable is given by

$$N = \frac{C}{r^D} \text{ or } \frac{N_2}{N_1} = \left(\frac{r_1}{r_2}\right)^D, \qquad (1)$$

where N is the number of objects associated with the size r, C is a constant, and D is the fractal dimension. A power law (Prieto) geostatistical distribution is generally a fractal.

One of the best examples of a fractal is the classic Koch triadic island illustrated in Figure 1. At the largest scale r_1, the triangle has three sides, $N_1 = 3$. At the next smaller scale, three triangles with sides $r_2 = r_1/3$ are added; there are now twelve sides, $N_2 = 12$. The construction can be continued indefinitely to smaller and smaller scales. The fractal dimension of this construction is easily obtained from equation 1 by taking its logarithm and writing it in the form

$$D = \frac{\ln (N_2/N_1)}{\ln (r_1/r_2)} = \frac{\ln 4}{\ln 3} = 1.262 \qquad (2)$$

Two important points should be made:

1. The Koch triadic island is scale invariant. The sides are self-similar at any magnification. It is impossible to tell the scale from a photograph of the island. Scale invariance is a characteristic of many geologic features; it is well known to every geologist who has ever looked at a picture of a rock formation without a rock hammer or lens cap to show the scale and could not figure out the size.

2. The length of the perimeter of the island approaches infinity as the construction is extended to smaller and smaller scales. This is the reason that the fractal dimension is greater than unity, the Euclidean dimension of a line. The length of the perimeter P is given by

$$P = Nr = Cr^{1-D}, \qquad (3)$$

where N has been substituted from equation 1.

The length of the perimeter of the Koch triadic island is analogous to the length of a rocky coastline. It was in this context that Mandelbrot (1967) introduced the concept of fractals. The length of the coastline obtained using a measuring rod of a specified length is plotted against the length of the measuring rod. The results for the west coast of Great Britain,

Fractals *continued on p. 3*

ISSN 1052-5173

SECOND CLASS
Postage Paid
at Boulder, Colorado
and at additional mailing offices

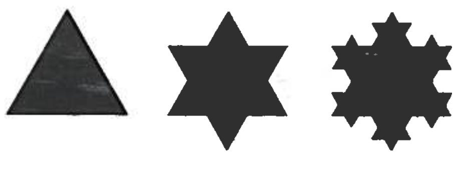

Figure 1. Three scales of the triadic Koch island, a classic fractal. At each smaller scale, triangles with sides one-third smaller are added to the center of each side of the larger scale. As the construction is carried to an infinitely smaller scale, the perimeter of the island has an infinite length, but its area is finite.

Fractals *continued from p. 1*

originally considered by Mandelbrot (1967), are given in Figure 2. The value $D = 1.25$ is typical for coastlines or topographic contours in a wide range of geologic provinces; it is also quite close to the value for the Koch triadic island. The length of a rocky coastline cannot be determined; the fractal dimension is a measure of its tortuosity.

The concept of fractals is easily introduced in an introductory physical geology course. When topographic maps are first considered the student can be asked to measure the total length along a specified contour using different spacings on a divider. The length of the contour (perimeter) is plotted against the divider length on log-log paper; from equation 3 the slope is 1-*D* and the fractal dimension of the contour can be obtained.

Self-similar Fractals

In many geological contexts the fractal distribution, equation 1, can be considered to be a statistical distribution. It is the only statistical distribution that is scale invariant; thus there is an underlying basis for its applicability to many geological problems. A few examples of self-similar fractals:

1. The Korcak relation for the number of islands with an area greater than a specified value is a fractal with $D = 1.30$ (Mandelbrot, 1975).

2. Cargill et al. (1980, 1981) have suggested that the fractal (power law) relation can be applied to the relation between tonnage and grade in economic ore deposits (Turcotte, 1986a).

3. Ivanhoe (1976) has suggested that the fractal (power law) relation can be applied to the number-size statistics for oil fields. It should be noted that log-normal statistics are often applied, but log-normal statistics are not scale invariant.

4. Earthquakes have a fractal relation between size and frequency of occurrence. Gutenberg and Richter (1954) established an empirical relation for the number of earthquakes *N* occurring in a specified length of time with magnitudes greater than *m* of the form

$$\log N = -bm + a, \qquad (4)$$

where a and b are constants. This relation is valid both globally and regionally, and the b value is usually near 0.9. Aki (1981) showed that equation 4 is a fractal relation equivalent to equation 1; when the magnitude *m* is converted to the rupture area r^2, the result is the simple relation

$$D = 2b. \qquad (5)$$

Thus, $D \approx 1.8$ for seismicity. The regional fractal distribution of seismicity may be used to assess the seismic hazards (Turcotte, 1989). The frequency of small earthquakes can be extrapolated to determine the frequency of occurrence of large earthquakes.

5. McClelland et al. (1989) have published frequency-volume statistics for volcanic eruptions that correlate well with equation 1, taking $D = 2.14$.

6. Materials can be fragmented in a variety of ways: naturally, by impacts, by explosives. Under many circumstances a fractal distribution as defined by equation 1 results (Turcotte, 1986b). The classic example for broken coal in Britain obtained by Bennett (1936) is given in Figure 3; good agreement with equation 1 is obtained taking $D = 2.50$.

It should be noted that empirical applications of fractals such as that illustrated in Figure 3 have upper and lower limits. The upper limit is the size of the largest fragment and generally is of the order of the size of the region fragmented; the lower limit is generally of the order of the grain size.

A simple model illustrates how fragmentation can result in a fractal distribution. This model is illustrated in Figure 4; at each scale two diagonally opposed blocks are retained and no two blocks of equal size are in direct contact with each other. This is the comminution model for fragmentation proposed by Sammis et al. (1986). It is based on the hypothesis that the direct contact between two fragments of nearly equal size will result in the breakup of one of the fragments. It is unlikely that a small fragment will break a large fragment or that a large fragment will break a small fragment. For the cube of dimension *h* illustrated in Figure 4 we have $N_1 = 2$ for $r_1 = h/2$ and $N_2 = 12$ for $r_2 = h/4$; thus, from equation 1 we have $D = \ln 6/\ln 2 = 2.5850$. Many fractal distributions of fragments have fractal dimensions near this value; one example was given in Figure 3; another is fault gouge (Sammis and Biegel, 1989).

The comminution model may also be applicable to tectonic fragmentation. It is probably a good approximation to assume that each fault has a characteristic earthquake. Thus the fractal frequency-magnitude statistics for earthquakes implies fractal number-size statistics for faults. Because of lack of exposure, erosion, and other effects it is in general difficult to quantify directly the number-size statistics of faults. A systematic study of the statistics of exposed joints and fractures has been given by Barton and Hsieh (1989). Basement rock near Yucca Mountain, Nevada, was cleared and the distribution of fractures mapped. Fractal dimensions near $D = 1.7$ were obtained; this compares with $D = 1.6$ for the surface exposure of the comminution model illustrated in Figure 4.

Self-affine Fractals

The ruler method for determining the fractal dimension of a rocky coastline was discussed in the previous section. An equivalent method is to determine the number of square boxes *N* of size *r* required to cover the coastline. If the dependence of *N* on *r* satisfies equation 1 a self-similar fractal is defined. In many cases, however, it is appropriate to use rectangular rather than square boxes. A noisy time series is a specific example. If the number of rectangular boxes of various sizes required to cover the time series satisfies equation 1 a self-affine fractal is defined.

Topography is an example of both self-similar and self-affine fractals. As discussed above a topographic map is usually an example of a self-similar fractal. A cross-section of topography with elevation plotted against position along a linear track is not a self-similar fractal, however; it is usually a self-affine fractal.

Spectral methods are generally applied to self-affine fractals. Consider the Fourier sine series for the height of topography *h*(*x*) along a linear track of length *L*. The Fourier representation is

$$h(x) = \sum_{n=1}^{\infty} A_n \sin\left(2\pi n x/L\right), \qquad (6)$$

where *L* is the length of the track and A_n is the amplitude associated with the wavelength

$$\lambda_n = \frac{L}{n}, \qquad (7)$$

with $n = 1, 2....$ The profile is a fractal if the amplitude coefficients A_n have a power law dependence on the wavelength λ_n, that is

$$A_n = C\,\lambda_n^{\frac{5-2D}{2}}, \qquad (8)$$

where C is again a constant. This relation is derived by counting the number of rectangular boxes of various sizes that are required to cover the profile (Voss, 1988).

As a specific example of a self-affine fractal, consider the random walk illustrated in Figure 5. Take a step forward and flip a coin; if it is heads take a step to the right; if it is tails, take a step to the left; take another step forward and repeat the process; this is Brownian noise. The amplitude of the noise depends on the length of the step to the side compared to the length of the step forward. For Brownian noise $D = 3/2$ and from equation 8 $A_n = C\,\lambda_n$; the amplitude is proportional to the wavelength. Brownian noise is a good statistical approximation to topography and bathymetry (Bell, 1975).

A global spectral expansion of topography and bathymetry has been carried out by Rapp (1989); his results are given in Figure 6. It is seen that equation 8 with $D = 1.5$ and $A_n = 10^{-4}\lambda_n$ is in good agreement with the data at all but the longest wavelengths. The fractal dimension of topography is

Fractals *continued on p. 4*

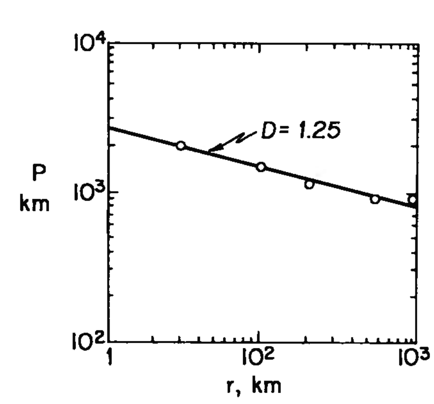

Figure 2. The open circles give the length *P* of the west coast of Great Britain as a function of the length of the measuring rod *r* (Mandelbrot, 1967). The solid line is equation 3 with the fractal dimension $D = 1.25$.

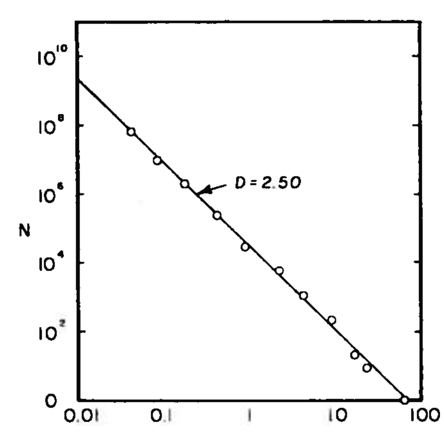

Figure 3. The number of pieces *N* of broken coal larger than a specified size *r* (Bennett, 1936) obtained by a sieve analysis. The line is equation 1 with the fractal dimension $D = 2.50$

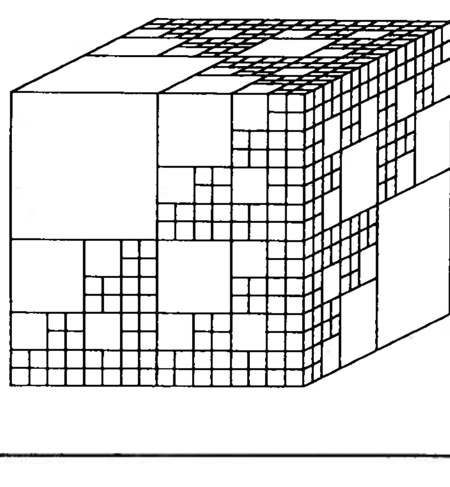

Figure 4. Fractal model for the comminution of a cube. Two large blocks are placed diagonally opposite each other at all scales. There are two blocks with $r = h/2$ and twelve blocks with $r = h/4$; thus, $D = \ln 6/\ln 2 = 2.58$.

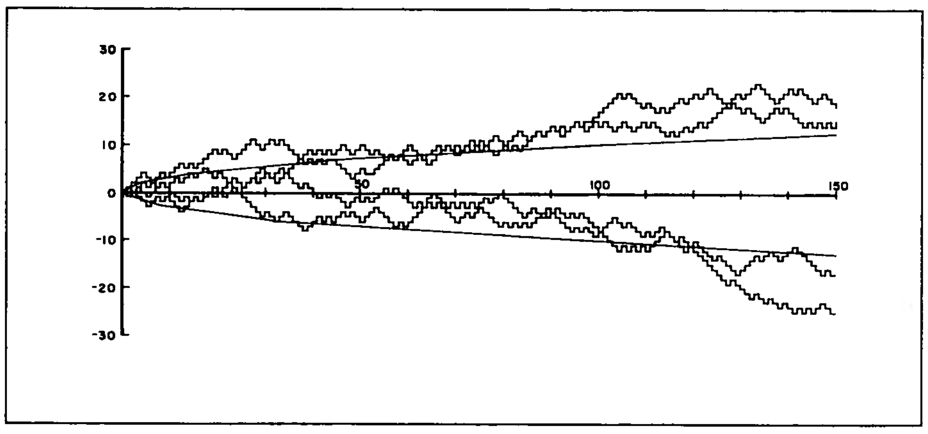

Figure 5. The zig-zag lines are four examples of a random walk (Brownian noise). The solid lines ($y = \sqrt{x}$) represent the mean dispersion of the walk.

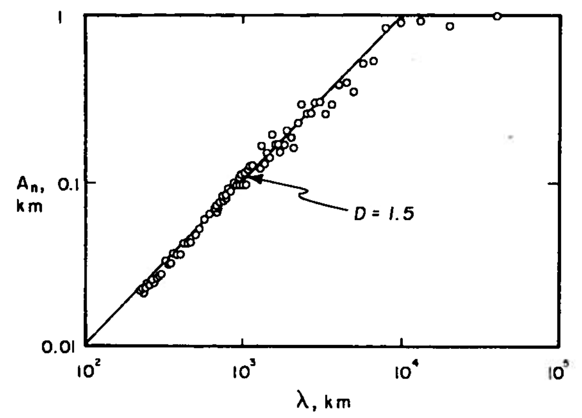

Figure 6. Dependence of amplitude coefficients A_n on the wavelengths λ_n for Earth's topography (Rapp, 1989).

Fractals *continued from p. 3*

generally near $D = 1.5$, but the amplitude is quite variable, being a measure of the roughness of the topography. The front-page photographs give maps of color-coded topography and color-coded roughness of the state of Arizona (Huang and Turcotte, 1989). The fractal dimension and roughness amplitude were obtained for each 4.5 × 4.5 km subregion in the state. The mean fractal dimension for linear tracks is $D = 1.50 \pm 0.10$. The roughness maps of Arizona clearly illustrate the erosional terrain associated with the Grand Canyon in northwest Arizona and the roughness contrasts between the basins (smooth) and ranges (rough) in southwest Arizona. There is very little variation in the fractal dimension between different types of topography; both the Grand Canyon and the Idaho batholith have fractal dimensions near 1.5.

What are Fractals Good for?

Another question I am often asked is "What are fractals good for?" The short answer is that they provide a means of quantifying scale-invariant processes. Because geology is filled with scale-invariant processes, there are many applications, some of which have been described above. But the answer is broader than this. In parallel with the concept of fractals, the concept of chaos has evolved in the past decade. Chaos and fractals are intimately connected; solutions that exhibit chaotic behavior invariably satisfy fractal statistics (Devaney, 1988).

Fractals can be useful strictly on an empirical basis. Power-law (fractal) statistics have been applied to a variety of geological problems; examples include petroleum and ore reserves. If the underlying physical and chemical processes are scale invariant, then the fractal distribution must be applicable.

Self-affine fractals are also applicable to a variety of problems on an empirical basis. Consider the problem of making a bathymetric chart when depths are known accurately along ship tracks. The bathymetry for a region can be expanded in a Fourier series in two directions. It is necessary to determine the amplitudes and phases for each harmonic. However, from the discussion given above, it is generally reasonable to assume that the amplitudes obey the fractal distribution given in equation 8. The data along the ship tracks are then used to specify the phases. The result is far more accurate than a brute-force fit or the results obtained by interpolation.

Hewett (1986) has used this technique to obtain the three-dimensional porosity structure of an oil field. Fractal statistics were used to interpolate between the porosity data for the existing wells. Remarkably realistic geologic structures were obtained; their accuracy was subsequently verified in a secondary recovery test.

Although empirical applications can be useful, fractals are often the result of chaotic processes. The definition of chaos is that two solutions with slightly different initial conditions diverge exponentially as they evolve. It is generally accepted that fluid turbulence is an example of deterministic chaos; the equations are well known and are relatively simple, but turbulence is complex and must be treated statistically. Since atmospheric flows are turbulent, weather and climate are examples of deterministic chaos.

There is also accumulating evidence that the tectonic deformation of Earth's crust is an example of deterministic chaos. The strike-slip behavior of blocks pulled along a surface is a simple analog to earthquakes. Huang and Turcotte (1990) showed that an asymmetrical pair of sliding blocks exhibits classical chaotic behavior. Carlson and Langer (1989) showed that a large number of identical sliding blocks behave chaotically. Simple cellular automata models (Bak and Tang, 1989; Kadanoff et al., 1989) produce fractal statistics of failure resembling earthquakes and indicate that the crust may be in a state of "self-organized criticality."

Drainage patterns and topography are classic examples of fractals. Thus the equations governing erosion must be nonlinear. Linear equations such as the diffusion equation for erosion (Culling, 1960) cannot generate fractals. Newman and Turcotte (1990) have proposed a model for erosion resembling models for turbulence. This nonlinear model produces and maintains self-similar fractal topography.

If you have read this far you may be interested in learning more about fractals. The book by Mandelbrot (1982) is relatively easy reading and gives a very personalized view of fractal concepts, but it is not particularly useful in terms of applications. Probably the best overall treatment of fractals at an intermediate level is the book by Falconer (1990). The volume of *Pure and Applied Geophysics* edited by Mandelbrot and Scholz (1989) presents a variety of applications of fractals to problems in geology and geophysics; further applications will appear in a book edited by C. C. Barton and P. R. LaPointe.

References Cited

Aki, K., 1981, A probabilistic synthesis of precursory phenomena, *in* Simpson, D.W, and Richards, P.G., eds., Earthquake prediction: Washington, D.C., American Geophysical Union, p. 556–574.

Bak, P., and Tang, C., 1989, Earthquakes as a self-organized critical phenomenon: Journal of Geophysical Research, v. 94, p. 15,635–15,637.

Barton, C.C., and Hsieh, P.A., 1989, Physical and hydrologic-flow properties of fractures (28th International Geological Congress Field Trip Guidebook T385): Washington, D.C., American Geophysical Union, 36 p.

Bell, T.H., 1975, Statistical features of sea-floor topography: Deep-Sea Research, v. 22, p. 883–892.

Bennett, J.G., 1936, Broken coal: London Journal of the Institute of Fuel, v. 10, p. 22–39.

Cargill, S.M., Root, D.H., and Bailey, E.H., 1980, Resource estimation from historical data: Mercury, a test case: Journal of the International Association for Mathematical Geology, v. 12, p. 489–522.

Cargill, S.M., Root, D.H., and Bailey, E.H., 1981, Estimating usable resources from historical industry data: Economic Geology, v. 76, p. 1081–1095.

Carlson, J.M., and Langer, J.S., 1989, Mechanical model of an earthquake fault, Physical Reviews, v. A40, p. 6470–6484.

Culling, W.E.H., 1960, Analytical theory of erosion, Journal of Geology. v. 68, p. 336–344.

Devaney, R.L., 1988, Fractal patterns arising in chaotic dynamical systems, *in* Peitgen, H. D., and Saupe, D., eds., The science of fractal images: New York, Springer-Verlag, p. 137–167.

Falconer, K., 1990, Fractal geometry: Chichester, England, John Wiley, 288 p.

Gutenberg, B. and Richter, C.F., 1954, Seismicity of the Earth and associated phenomena [second edition]: Princeton, New Jersey, Princeton University Press, 310 p.

Hewett, T.A., 1986, Fractal distributions of reservoir heterogeneity and their influence on fluid transport: Society of Petroleum Engineers Paper 15386, 15 p.

Huang, J., and Turcotte, D.L., 1989, Fractal mapping of digitized images: Applications to the topography of Arizona and comparisons with synthetic images: Journal of Geophysical Research, v. 94, p. 7491–7495.

Huang, J., and Turcotte, D.L., 1990, Are earthquakes an example of deterministic chaos?: Geophysical Research Letters, v. 17, p. 223-226.

Ivanhoe, L.F., 1976, Oil/gas potential in basin estimates: Oil and Gas Journal, v. 6, p. 154–155.

Kadanoff, L.P., Nagel, S.R., Wu, L., and Zhou, S.M., 1989, Scaling and universality in avalanches: Physical Review, v. A39, p. 6524–6533.

Mandelbrot, B.B., 1967, How long is the coast of Britain? Statistical self-similarity and fractional dimension: Science, v. 156, p. 636–638.

Mandelbrot, B.B., 1975, Stochastic models for the earth's relief, the shape and the fractal dimension of the coastlines, and the number-area rule for islands: National Academy of Science Proceedings, v. 72, p. 3825–3828.

Mandelbrot, B.B., 1982, The fractal geometry of nature: San Francisco, Freeman, p. 460.

Mandelbrot, B.B., and Scholz, C.H., editors, 1989, Fractals in geophysics: Pure and Applied Geophysics, v. 131.

McClelland, S.T., Summers, M., Nielson, E., and Stein, T.C., editors, 1989, Global volcanism, 1975–1985: Englewood Cliffs, New Jersey, Prentice-Hall, 655 p.

Newman, W.I., and Turcotte, D.L., 1990, Cascade model for fluvial geomorphology: Geophysical Journal International, v. 100, p. 433–439.

Rapp, R.H., 1989, The decay of the spectrum of the gravitational potential of the Earth: Geophysical Journal International, v. 99, p. 449-455.

Sammis, C.G., and Biegel, R.L., 1989, Fractals, fault gouge, and friction: Pure and Applied Geophysics, v. 131, p. 255–271.

Sammis, C.G., Osborne, R.H., Anderson, J.L., Banerdt, M., and White, P., 1986, Self-similar cataclasis in the formation of fault gouge: Pure and Applied Geophysics, v. 123, p. 53–78.

Turcotte, D.L., 1986a, A fractal approach to the relationship between ore grade and tonnage: Economic Geology, v. 81, p. 1528–1532.

Turcotte, D.L., 1986b, Fractals and fragmentation: Journal of Geophysical Research, v. 91, p. 1921–1926.

Turcotte, D.L., 1989, A fractal approach to probabilistic seismic hazard assessment: Tectonophysics, v. 167, p. 171-177.

Voss, R.F., 1988, Fractals in nature: From characterization to simulation, *in* Peitgen, H.O., and Saupe, D., editors, The science of fractal images: New York, Springer-Verlag, p. 21–70. ■